

Origin of the low-temperature plasma in the Galactic center X-ray emission

Shigeo YAMAUCHI¹*, Miku SHIMIZU¹, Masayoshi NOBUKAWA², Kumiko K. NOBUKAWA¹, Hideki UCHIYAMA³, and Katsuji KOYAMA⁴

¹Department of Physics, Nara Women's University, Kita-uoyanishimachi, Nara 630-8506

²Faculty of Education, Nara University of Education, Takabatake-cho, Nara 630-8528

³Faculty of Education, Shizuoka University, 836 Ohya, Suruga-ku, Shizuoka 422-8529

⁴Department of Physics, Graduate School of Science, Kyoto University, Kitashirakawa-oiwake-cho, Sakyo-ku, Kyoto 606-8502

*E-mail: yamauchi@cc.nara-wu.ac.jp

Received ; Accepted

Abstract

The Galactic Center X-ray Emission (GCXE) is composed of high temperature (~ 7 keV) and low temperature (~ 1 keV) plasmas (HTP and LTP, respectively). The global structure of the HTP is roughly uniform over the Galactic center (GC) region, and the origin of the HTP has been extensively studied. On the other hand, the LTP is more clumpy, and the origin has not been studied in detail. In the S XV He α line map, a pair of horn-like soft diffuse sources are seen at the symmetric positions with respect to Sagittarius A*. The X-ray spectra of the pair are well represented by an absorbed thin thermal plasma model of a temperature and N_{H} of 0.6–0.7 keV and $4 \times 10^{22} \text{ cm}^{-2}$, respectively. The N_{H} values indicate that the pair are located near at the GC. Then the dynamical time scales of the pair are $\sim 10^5$ yr. The Si and S abundances and the surface brightnesses in the the S XV He α line band are 0.7–1.2 and 0.6–1.3 solar, and $(2.0\text{--}2.4) \times 10^{-15} \text{ erg s}^{-1} \text{ cm}^{-2} \text{ arcmin}^{-2}$, respectively. The temperature, abundances, and surface brightness are similar to those of the LTP in the GCXE, while the abundances are far larger than those of known point sources, typically coronal active stars and RS CVn-type active binaries. Based on these results, possible origin of the LTP is discussed.

Key words: Galaxy: center — X-rays: diffuse background — X-rays: soft diffuse sources

1 Introduction

The spectrum of the Galactic Diffuse X-ray Emission (GDXE) has strong K-shell transition lines of highly ionized atoms and neutral iron. The strongest are the He-like iron (Fe XXV He α) and sulfur (S XV He α) lines, which indicates that the GDXE is composed of a high-temperature plasma of ~ 7 keV (HTP) represented by the Fe XXV He α line, and a low-temperature plasma of ~ 1 keV (LTP) represented by the S XV He α line (Uchiyama et al. 2013). The other component is a power-law with the Fe I K α line. The equivalent widths and scale heights of the Fe XXV He α and Fe I K α lines are position dependent in the GDXE, and hence the GDXE is spatially and

spectrally separated into the Galactic Center X-ray Emission (GCXE), the Galactic Ridge X-ray Emission (GRXE), and the Galactic Bulge X-ray Emission (GBXE) (Yamauchi et al. 2016; Nobukawa et al. 2016; Koyama 2018).

A long standing question of the GDXE is its origin, whether it is integrated emission of point sources, diffuse plasma, or else. Using the deep Chandra observation in the 6.5–7.1 keV band, Revnivtsev et al. (2009) and Hong (2012) made an X-ray Luminosity Function (XLF: the integrated flux of point sources as a function of the point source flux) down to the luminosity of $\sim 4 \times 10^{29} \text{ erg s}^{-1}$, and resolved more than 80 % flux of the GBXE into point sources. However, the profiles of the XLF

and integrated spectra of the point sources were largely different between these authors, which led different prediction of the point source composition in the GBXE: RS-CVn type active binaries (ABs) and cataclysmic variables (CVs) with the mixing ratio of $\sim 2:1$ (Revnivtsev et al. 2009), or CVs dominant (Hong 2012). A possibility of these mismatch in the mixing ratio of point sources would be that the authors ignore the energy band difference of the compositions; they simply referred the XLF results in the 6.5–7.1 keV band (HTP), not the full energy band of the HTP and LTP. Using the spectrum difference of ABs, CVs, and GBXE in the 5–10 keV band, Nobukawa et al. (2016) suggested that the GBXE is composed of ABs and CVs with the mixing ratio of $\sim 3:7$. In the full energy band (1–10 keV), the compositions would not be only these point sources (ABs and CVs), but may include true diffuse plasma or even unknown objects. Therefore, the simple point source origin should be carefully re-examined for the HTP and LTP in a proper mixture of these two components.

This paper utilizes the GCXE for the study of the LTP origin, because more reliable spectra would be available due to the surface brightness of ~ 10 times larger than the GBXE and GRXE. We reports properties of a pair of soft diffuse sources NE and NW in the LTP map at the northeast and northwest of the Galactic center (GC). The diffuse sources have been noted by Wang et al. (2002) (Chandra) and Ponti et al. (2015) (XMM-Newton), but the detailed information has not been reported. Based on the improved spectral and spatial information of Suzaku, the origin of NE and NW, and possible interpretation of the origin of the LTP in the GCXE are discussed. Throughout this paper, the distance to the GC is 8 kpc (e.g., Reid 1993; Gillessen et al. 2009), and quoted errors are in the 90% confidence limits.

2 Observations

Survey observations in the GC region were carried out with the X-ray Imaging Spectrometer (XIS; Koyama et al. 2007) onboard Suzaku (Mitsuda et al. 2007). This paper utilized these Suzaku data in the archive. The XISs were composed of 4 CCD cameras placed on the focal planes of the thin foil X-ray Telescopes (XRT; Serlemitsos et al. 2007). XIS 1 was a back-side illuminated (BI) CCD, while XIS 0, 2, and 3 were front-side illuminated (FI) CCDs. The field of view (FOV) of the XIS was 17.8×17.8 . The data from the three sensors (XIS 0, 1, and 3) were used for most of the observations, because XIS 2 stopped working in 2006 November. Since the spectral resolution of the XIS was degraded due to the radiation of cosmic particles, the spaced-row charge injection (SCI) technique was applied to restore the XIS performance (Uchiyama et al. 2009). After removing hot and flickering pixels, we used the data of the ASCA grade 0, 2, 3, 4, and 6.

3 Analysis and results

The XIS pulse-height data are converted to Pulse Invariant (PI) channels using the `xispi` software in the HEASoft 6.19 and the calibration database version 2016-06-07. The data in the South Atlantic Anomaly, during the earth occultation, and at the low elevation angle from the earth rim of $< 5^\circ$ (night earth) and $< 20^\circ$ (day earth) are excluded. Figure 1 shows the results of the Suzaku GC survey, covering the full area of the GC by multiple pointings. The non X-ray background (NXB), estimated using `xisnxbgen` (Tawa et al. 2008), is subtracted. To highlight the contrast between the HTP and LTP distributions, X-ray images of the Fe XXV He α (6.55–6.8 keV) and S XV He α (2.3–2.6 keV) bands are separately made. A pair of soft diffuse sources (NE and NW) are detected in two fields of the XIS. The observation logs of the two fields, which include the pair sources NE and NW, and background (BGD), are given in table 1.

3.1 Overview of soft diffuse sources in the GCXE

In the Fe XXV He α line map (HTP distribution), some slightly enhancement are found near at the giant molecular cloud complex (GMC) of Sagittarius (Sgr) A, Sgr C, and Arches cluster (blue dashed lines in figure 1a). The Fe XXV He α line enhancement is about $\sim 10\%$ of the GCXE level. Thus global distribution of the HTP is smooth in the full area of the GC. In the LTP distribution, on the other hand, the S XV He α image shows a largely extended X-ray emission near at $(l, b) \sim (0.3, 0.4)$ (GC North, Nakashima et al. 2014). The spectrum of this soft diffuse source is in collisional ionization equilibrium (CIE) with a temperature of 0.81 keV and solar abundances. Another soft diffuse source is a super bubble candidate (G359.79–0.26 and G359.77–0.09) found by Mori et al. (2008), Mori et al. (2009), and Heard & Warwick (2013), whose spectra are explained by an absorbed thermal plasma model in CIE with temperatures of ~ 1.0 and ~ 0.7 keV, and abundances of 1.1–1.7 and 1.0–1.4 solar, respectively. A notable soft diffuse source is found around the Sgr A X-ray reflection nebula (XRN) near Sgr A* (near XRN complex), firstly reported by Park et al. (2004). This source has different morphology in the Fe XXV He α image, slim and faint, which corresponds to the GMC complex (named, Sgr A GMC), or Sgr A XRN. For this source, however, no spectral information has been available. Other soft diffuse sources are found near the Sgr C GMC (the Chimney and G359.41-0.12), firstly reported by Tsuru et al. (2009). The temperatures are ~ 1.2 and ~ 0.9 keV with abundances of ~ 1.7 solar. In addition to these soft diffuse sources, we can see a pair of horn-like diffuse sources NE and NW, at the north (in the Galactic coordinate) of the GC.

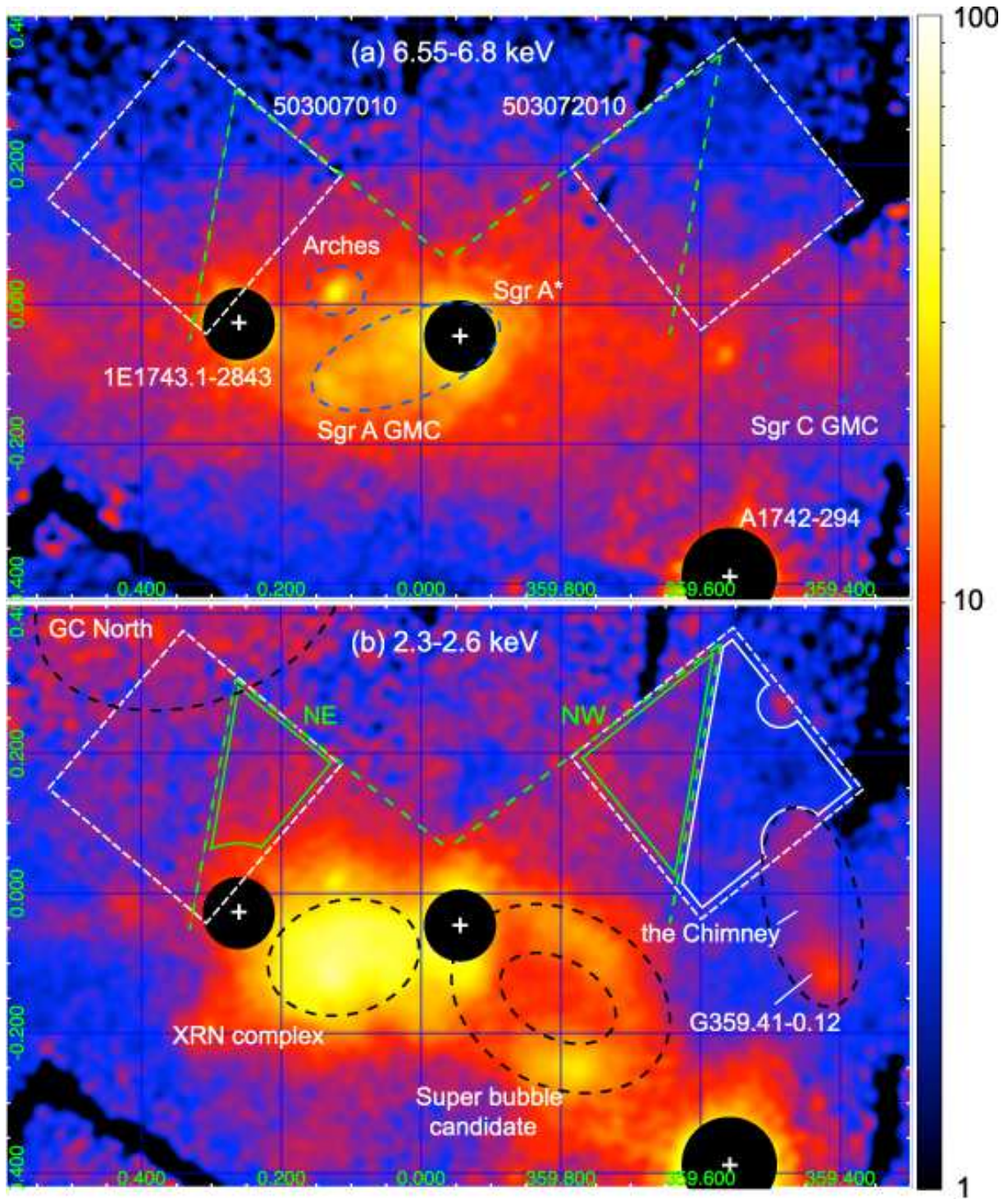


Fig. 1. XIS images in the (a) 6.55–6.8 (Fe XXV He α) and (b) 2.3–2.6 keV (S XV He α) bands in the Galactic coordinate. The color bar shows surface brightness in the logarithmic scale. The unit is 2×10^{-13} erg s $^{-1}$ cm $^{-2}$ arcmin $^{-2}$ for (a) and 1×10^{-13} erg s $^{-1}$ cm $^{-2}$ arcmin $^{-2}$ for (b). Bright point sources are masked by the black circles. A stray-light region of the brightest source A1742–294 is given by the large black circle. The white dashed squares, the solid lines and the green horn-like lines indicate the XIS FOVs, the background region (BGD), and a pair of soft diffuse sources (NE and NW), respectively. The black dashed lines in (b) outline other LTP clumps, while the blue dashed lines in (a) are the regions of HTP clumps. In order to figure out the difference between the HTP and LTP structure, the XIS FOVs and horn-like structures in the LTP are also shown in the HTP image.

Observation ID	Pointing Position (l, b)	Observation time (UT) Start – End	Exposure time (ks)	Region*
503007010	(0°3285, +0°1690)	2008-09-02 10:15:27 – 2008-09-03 22:52:24	52.2	NE
503072010	(359°5753, +0°1669)	2009-03-06 02:39:12 – 2009-03-09 02:55:25	140.6	NW, BGD

* See figure 1.

3.2 X-ray spectra of soft diffuse sources, NE and NW

The X-ray spectra of NE and NW after the subtraction of the NXB (see section 2) are made from the source regions. The BGD region is selected from a nearby blank sky of similar Galactic latitude to those of NE and NW. The X-ray spectrum of BGD is made with the same process as NE and NW. In order to make the spectra of NE, NW, and BGD with good statistics, we utilize the two XIS fields, which include a large fraction of NE, NW, and BGD with long exposure times (table 1). The flux of the NXB are $\sim 9\%$ and $\sim 14\%$ of the total counts of the background region (BGD) in the 1–8 keV band for FI and BI, respectively, and the statistical error is less than 1%. Thus, the uncertainty caused by the NXB subtraction is not significant in the following spectral analysis. The flux of the BGD spectrum is fine-tuned, taking account of the longitude and latitude differences between BGD and the pair sources (NE and NW) and using the e-folding longitude and latitude scales of the GCXE of 0°63 and 0°26, respectively (Uchiyama et al. 2013; Yamauchi et al. 2016; Koyama 2018). The fine-tuning factor is 1.3 for NE and 1.1 for NW. Then, the BGD spectrum multiplied by this fine-tuning factor is subtracted from the NE and NW spectra. The resultant NE and NW spectra are shown in figure 2, in which many emission line features are found. In order to increase photon statistics, the spectra with the FI sensors (XIS 0 and 3) are co-added, but the XIS 1 spectrum is treated separately, because the response functions of the FIs and BI are different. Response files, Redistribution Matrix Files (RMFs) and Ancillary Response Files (ARFs) are made using `xisrmfgen` and `xissimarfgen` (Ishisaki et al. 2007), respectively. The abundance tables, and the atomic data of the lines and continua of the thin thermal plasma are taken from Anders & Grevesse (1989) and ATOMDB 3.0.9, respectively.

The NE and NW spectra are fitted with a CIE plasma model of solar abundances, `vapex` in XSPEC version 12.9.0u. This model is rejected ($\chi^2/\text{d.o.f.}$ of 163/119 and 177/119, respectively) with residuals at the Si, S, and Ar lines. Therefore, the NE and NW spectra are re-fitted by the same CIE model, but the abundances of Si, S, and Ar (=Ca) are treated as free parameters. Then an improved fit is obtained with $\chi^2/\text{d.o.f.}$ of 147/116 and 158/116, respectively¹. The best-fit model is shown in fig-

¹ Exactly speaking, this model is not accepted from the statistical point of

Table 2. The best-fit parameters of NE and NW.

Parameter	Value	
	NE	NW
N_{H} (cm^{-2})	$(4.4^{+0.3}_{-0.4}) \times 10^{22}$	$(4.2^{+0.6}_{-0.2}) \times 10^{22}$
kT_e (keV)	$0.64^{+0.11}_{-0.07}$	$0.71^{+0.06}_{-0.12}$
Si* (Solar)	$0.7^{+0.3}_{-0.2}$	1.2 ± 0.3
S* (Solar)	$0.6^{+0.3}_{-0.2}$	1.3 ± 0.3
Ar=Ca* (Solar)	2.3 ± 1.1	$3.3^{+1.2}_{-1.1}$
Others* (Solar)	1 (fixed)	1 (fixed)
Normalization [†]	$(4.0^{+2.2}_{-1.5}) \times 10^{-4}$	$(1.7^{+1.6}_{-0.4}) \times 10^{-4}$
$\chi^2/\text{d.o.f.}$	147/116	158/116

* Abundance relative to the solar value (Anders & Grevesse 1989).

[†] Defined as $10^{-14} \times \int n_{\text{H}} n_e dV / 4\pi D^2 \Omega$ ($\text{cm}^{-5} \text{ arcmin}^{-2}$), where n_{H} , n_e , D and Ω are hydrogen density (cm^{-3}), electron density (cm^{-3}), distance (cm) and solid angle (arcmin^2) of the source, respectively.

ure 2, while the best-fit parameters are given in table 2. The flux in the S XV He α line band (2.3–2.6 keV) are $2.4 \times 10^{-15} \text{ erg s}^{-1} \text{ cm}^{-2} \text{ arcmin}^{-2}$ for NE and $2.0 \times 10^{-15} \text{ erg s}^{-1} \text{ cm}^{-2} \text{ arcmin}^{-2}$ for NW.

4 Discussion

Chandra found many point sources in the GC region (e.g., Muno et al. 2009). The flux of the integrated point sources in the regions of NE and NW is only $\sim 10\%$, and hence the contribution of the resolved point sources for NE and NW would be negligible. The surface brightness of NE and NW is nearly the same level of the nearby GCXE. The N_{H} values of the pair sources, NE and NW, are $\sim 4 \times 10^{22} \text{ cm}^{-2}$ (table 2), roughly consistent with those of the point sources located at the GC region (Sakano 2000; Sakano et al. 2002). Therefore, here and after, we assume that NE and NW are located near the GC region at the distance of 8 kpc.

The pair of soft diffuse sources, NE and NW, have horn-like structures standing above the Galactic plane (see, figure 1b).

view, which may be due to systematic errors caused in the BGD subtraction process. Taking account of the possible systematic errors, we regard the model is a good approximation of the NE and NW spectra.

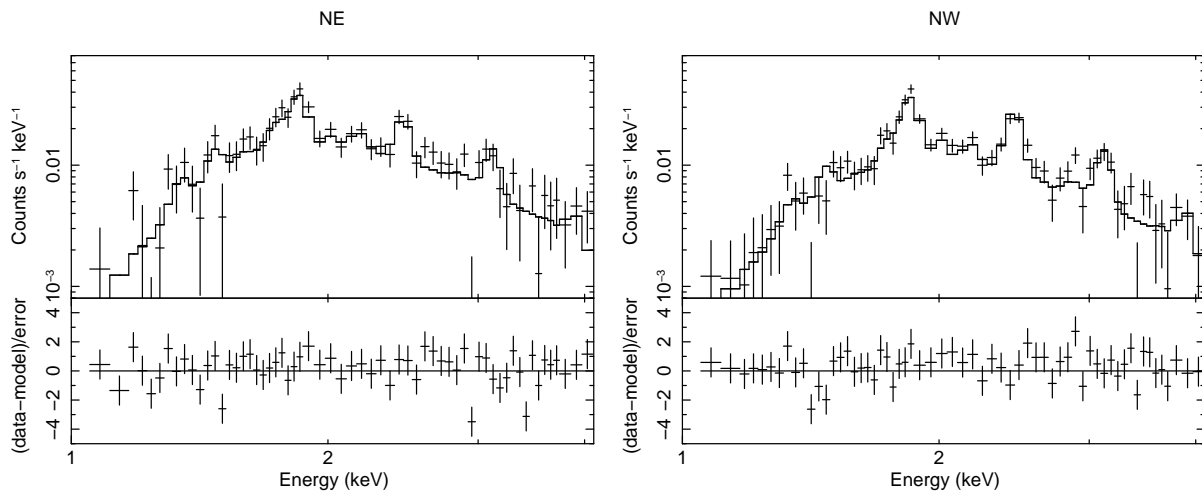


Fig. 2. X-ray spectra of NE and NW (upper panels) and the residuals from the best-fit model (lower panels). Only the spectra obtained with the FI sensors in the 1–4 keV band are displayed for brevity.

Assuming a cone shape geometry with a diameter of the base of $\sim 15'$ (35 pc) and a height of $\sim 15'$, the volume (V) is estimated to be $V = 3.3 \times 10^{59} \text{ cm}^3$. Using the best-fit volume emission measure, and assuming a filling factor = 1 and $n_e = 1.2n_H$, where n_e and n_H are the electron and hydrogen densities, respectively, we obtain the mean hydrogen density (n_H), the thermal energy (E_{th}), gas mass (M_{gas}), and sound velocity (c_s) for NE to be $n_H = 0.3 \text{ cm}^{-3}$, $E_{\text{th}} = 3 \times 10^{50} \text{ erg}$, $M_{\text{gas}} = 120 M_{\odot}$, and $c_s = 4 \times 10^7 \text{ cm s}^{-1}$. For NW, we obtained $n_H = 0.2 \text{ cm}^{-3}$, $E_{\text{th}} = 2 \times 10^{50} \text{ erg}$, $M_{\text{gas}} = 80 M_{\odot}$, and $c_s = 4 \times 10^7 \text{ cm s}^{-1}$. The dynamical time scale (t_{dyn}) is estimated to be $t_{\text{dyn}} \simeq 1 \times 10^5 \text{ yr}$.

Most of these physical parameters of NE and NW are consistent with those of middle-aged SNRs. However, the plasma size is larger than typical middle-aged SNRs, and the horn-like morphology is largely different from that of a single SNR. The physical parameters and the dynamical time scales of NE and NW are similar to each other, and the pair positions are symmetric with respect to Sgr A*. These suggest that the pair, NE and NW, originated from the same event, possibly a past activity in the GC region.

Remarkable features in the LTP map are the presence of many bright soft diffuse sources (Mori et al. 2008; Mori et al. 2009; Tsuru et al. 2009; Heard & Warwick 2013; Nakashima et al. 2014; Ponti et al. 2015), including NE and NW, near the GC. These soft diffuse sources have similar temperature and Si–S abundances to those of the LTP in the GCXE (Uchiyama et al. 2013). In the scenario of the point source origin for the LTP, a candidate source in the luminosity range of $> 10^{30} \text{ erg s}^{-1}$ has been regarded to be ABs with a thermal spectrum of temperature $\gtrsim 1 \text{ keV}$ (Sazonov et al. 2006; Warwick 2014). However, the fraction of the resolved point sources of the GCXE in this luminosity range is less than a few 10% (Muno et al. 2003; Revnivtsev et al. 2007). Therefore, the major con-

tribution of point sources should come from the lowest luminosity range of $\sim 10^{28} - 10^{30} \text{ erg s}^{-1}$. In this luminosity range, the candidate source may not be only ABs, but includes coronal active stars (CAs) with the temperature of $\lesssim 1 \text{ keV}$ (e.g., Güdel 2004; Pandey & Singh 2008). In this case, the number of required point sources is more than $\sim 10^5 - 10^6$, because the total LTP luminosity of the GCXE is $\sim 10^{36} \text{ erg s}^{-1}$ (Uchiyama et al. 2013). Since this huge number of point sources would lead a uniform LTP distribution, the presence of many bright soft diffuse sources disfavors the point source origin.

Most of the soft diffuse sources have dynamical time scales of $\sim 10^5 \text{ yr}$, which corresponds to the last epoch of the high star formation activity of $\sim 10^5 - 10^7 \text{ yr}$ ago (Yusef-Zadeh et al. 2009). The abundances of Si and S of NE and NW and most of other soft diffuse sources are larger than CAs (typically ~ 0.2 solar, e.g., Pandey & Singh 2008), but are typical to those of a normal diffuse hot plasma. The horn-like sources NE and NW may be made by either super-wind from multiple supernovae, high activity of stellar wind from many high-mass stars in the GC region $\sim 10^5 \text{ yr}$ ago (Ponti et al. 2015), or the past flares of Sgr A* (e.g., Koyama 2018). The origin of a power-law component with the Fe I $K\alpha$ line (6.4 keV) would also be the same activities near the GC.

Acknowledgement

The authors are grateful to all members of the Suzaku team. KKN is supported by Research Fellowships of JSPS for Young Scientists. This work was supported by the Japan Society for the Promotion of Science (JSPS) KAKENHI Grant Numbers JP24540232 (SY) and JP16J00548 (KKN).

References

- Anders, E., & Grevesse, N. 1989, *Geochim. Cosmochim. Acta*, 53, 197
- Gillessen, S., Eisenhauser, F., Trippe, S., Alexander, T., Genzel, R., Martins, F., & Ott, T. 2009, *ApJ*, 692, 1075
- Güdel, M. 2004, *A&A review*, 12, 71
- Heard, V., & Warwick, R. S. 2013, *MNRAS*, 434, 1339
- Hong, J. 2012, *MNRAS*, 427, 1633
- Ishisaki, Y., et al. 2007, *PASJ*, 59, 113
- Koyama, K., et al. 2007, *PASJ*, 59, S23
- Koyama, K. 2018, *PASJ*, 70, 1
- Mitsuda, K., et al. 2007, *PASJ*, 59, S1
- Mori, H., Tsuru, T. G., Hyodo, Y., Koyama, K., & Senda, A. 2008, *PASJ*, 60, 183
- Mori, H., Hyodo, Y., Tsuru, T. G., Nobukawa, M., & Koyama, K. 2009, *PASJ*, 61, 687
- Muno, M. P., et al. 2003, *ApJ*, 589, 225
- Muno, M. P., et al. 2009, *ApJS*, 181, 110
- Nakashima, S., Nobukawa, M., Uchida, H., Tanaka, T., Tsuru, T. G., Koyama, K., Murakami, H., & Uchiyama, H. 2013, *ApJ*, 773, 20
- Nakashima, S., Nobukawa, M., Uchida, H., Tanaka, T., Tsuru, T. G., Koyama, K., Uchiyama, H., & Murakami, H. 2014, *Proceedings of the International Astronomical Union*, Vol. 303, 349
- Nobukawa, M., Uchiyama, H., Nobukawa, K. K., Yamauchi, S., & Koyama, K. 2016, *ApJ*, 833, 268
- Pandey, J. C., & Singh, K. P. 2008, *MNRAS*, 387, 1627
- Park, S., Muno, M. P., Baganoff, F. K., Maeda, Y., Morris, M., Howard, C., Bautz, M. W., & Garmire, G. P. 2004, *ApJ*, 603, 548
- Ponti, G., et al. 2015, *MNRAS*, 453, 172
- Reid, M. J. 1993, *ARA&A*, 31, 345
- Revnivtsev, M., Vikhlinin, A., & Sazonov, S. 2007, *A&A*, 473, 857
- Revnivtsev, M., Sazonov, S., Churazov, E., Forman, W., Vikhlinin A., & Sunyaev, R. 2009, *Nature*, 458, 1142
- Sakano, M. 2000, Ph. D. thesis, Kyoto University
- Sakano, M., Koyama, K., Murakami, H., Maeda, Y., & Yamauchi, S. 2002, *ApJS*, 138, 19
- Sazonov, S., Revnivtsev, M., Gilfanov, M., Churazov, E., & Sunyaev, R. 2006, *A&A*, 450, 117
- Serlemitsos, P., et al. 2007, *PASJ*, 59, S9
- Tawa, N., et al. 2008, *PASJ*, 60, S11
- Tsuru, T. G., Nobukawa, M., Nakajima, H., Matsumoto, H., Koyama, K., Yamauchi, S. 2009, *PASJ*, 61, S219
- Uchiyama, H., et al. 2009, *PASJ*, 61, S9
- Uchiyama, H., Nobukawa, M., Tsuru, T. G., & Koyama, K. 2013, *PASJ*, 65, 19
- Wang, Q. D., Gotthelf, E. V., & Lang, C. C. 2002, *Nature*, 415, 148
- Warwick, R. S. 2014, *MNRAS*, 445, 66
- Yamauchi, S., Nobukawa, K. K., Nobukawa, M., Uchiyama, H., & Koyama, K. 2016, *PASJ*, 68, 59
- Yusef-Zadeh, F., et al. 2009, *ApJ*, 702, 178